International Journal of Systems Signal Control and Engineering Application

MEDWELL PUBLICATIONS

Performance Analysis of Local Binary Patterns in Texture Classification

Ch. Sudha Sree and M.V.P. Chandra Sekhara Rao
Department of CA and CSE, R.V.R&J.C College of Engineering, Guntur, India

Key words: Local Binary Patten (LBP), Local Ternary Pattern (LTP), Completed Local Binary Pattern (CLBP), Completed Local Binary Count (CLBC), Adjacent Evaluation Completed Local Binary Pattern (AECLBP), texture classification, rotation invariant

Corresponding Author:
Ch. Sudha Sree
Department of CA and CSE, R.V.R&J.C College of Engineering, Guntur, India

Page No.: 74-84
Volume: 12, Issue 4, 2019
ISSN: 1997-5422
International Journal of Systems Signal Control and Engineering Application

Abstract: This study presents a detailed comparative study on various Local Binary Pattern (LBP) variant texture descriptors in texture classification. The work includes nine various texture descriptor methods namely LBP^{riu2}, LBP^{ri}, LTP, VAR, LBP/VAR, CLBP, CLBC, AECLBP, AELTP. The performance of these methods is evaluated basing on three well-known benchmark texture databases OUTEX, CUReT, UIUC, using the nearest-neighbourhood classifier.

INTRODUCTION

Texture classification has an important role in image processing and computer vision applications such as character recognition (Tuceryan and Jain, 1993), rock classification (Lepisto *et al*., 2003), wood species recognition (Tou *et al*., 2009), face detection (Hen *et al*., 2007), fabric classification (Salem and Nasri, 2009), geographical landscape segmentation (Recio *et al*., 2005), image retrieval, remote sensing and medical image analysis. The texture classification methods can be categorized into statistical methods, model based methods and structural methods. The statistical methods are proposed, based on statistics selected features from spatial distribution of neighbouring pixels in an image such as polorograms with generalized co-occurrence matrices (Davis *et al*., 1979), texel property histogram (Goyal *et al*., 1995), Fourier descriptors (Duvernoy, 1984) and moment invariant methods (Hu, 1962). Model based approaches are developed based on probability model or linear combination of set of basic functions. The model based methods, for example are Circular Simultaneous Auto Regressive (CSAR) model (Kashyap and Khotanzad, 1986), steerable pyramid (Greenspan *et al*., 1994), Gaussian Markov random fields (Cohen *et al*., 1991). Structural methods are developed based on the well-defined primitives and spatial arrangements. The structural methods in the literature are topologically invariant texture method (Eichman and Kasparis, 1988), improved iterative morphological decomposition (Lam and Li, 1997). All these methods provide the texture classification either as rotation variant, or invariant and either noise sensitive or insensitive.

Local Binary Pattern (LBP) is a well-known method of texture classification and is a combination of structural and statistical approach. Various local binary pattern

methods are proposed in literature. These methods gain popularity due to their impressive classification accuracy on texture database. The Local Binary Pattern (LBP) (Ojala *et al*., 2002) is developed by Ojala *et al*. (2002). The two steps in local binary pattern are thresholding and encoding. In thresholding, local gray scale difference is computed with neighbourhood pixels around the selected centre pixel with radius R(1,2,3). The threshold value may be either one or zero, based on the difference value. The encoding step converts the bit pattern of threshold into decimal number. Though the LBP is a successful method in texture classification, it is sensitive to rotation and also has vast majority patterns. To overcome the disadvantage, Ojala *et al*. (2002) proposed a uniform local binary pattern with rotation invariance ($LBP^{riu2}_{P,\ R}$) (Ojala *et al*., 2002). It is used in different applications such as face recognition, shape localization (Huang *et al*., 2004). The uniform local binary pattern with rotation invariance ($LBP^{riu2}_{P,\ R}$) is invariant to gray scale difference. Thus, it rejects contrast of local image. So, contrast of image is provided by local Variance method (VAR) (Ojala *et al*., 2002) with rotation invariance and it is variant to gray scale difference. The joint distribution of local variance and $LBP^{riu2}_{P,\ R}$ (Ojala *et al*., 2002) provides significant classification accuracy than individual and VAR. Guo *et al*. (2010) developed a Completed Local Binary Pattern (CLBP) (Guo *et al*., 2010) for texture classification to improve the performance of classification accuracy when compared to LBP. CLBP is not totally rotation invariant. To overcome the disadvantage of CLBP, Zho *et al*. (2012) proposed a Completed Local Binary Count (CLBC) (Zho *et al*., 2012). Local binary pattern is not only rotation variant but also sensitive to noise. As a solution Local Ternary Pattern (LTP) (Taha and Triggs, 2010) is proposed by Tan and Triggs (2010) which is less sensitive to noise when compared to LBP. Another pitfall of LBP is it does not provide the dissimilarity between patterns. Completed Local Ternary Pattern (CLTP) is proposed by Taha and BeeEeKhoo with the extension of Local Ternary Pattern (LTP). Nishant Shrivastava and Tyagi (2014) developed a completed Local Structural Pattern (CLSP) with global information. But CLSP is sensitive to noise, thus, Shrivastava and Tyagi (2014) further developed robust local structural pattern (RLSP) and made the method as insensitive to noise. Itachieved good classification accuracy compared to CLBP and LBP. Adjacent Evaluation Local Binary Pattern (AELBP), Adjacent Evaluation Completed Local Binary Pattern (AECLBP) and Adjust Evaluation of Local Ternary Pattern (AELTP) are proposed by Song *et al*. (2015). These are robust to noise when compared to CLBP and LBP. In this study, we have studied the performance of these methods in classification using three benchmark data sets.

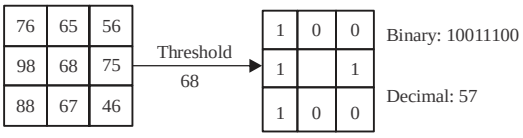

Fig. 1: Illustration of LBP operator

Literature review: The description of LBP is as follows:

Local Binary Pattern (LBP): LBP is a texture descriptor that characterizes the texture image using two steps, thresholding and encoding. Given a pixel of image, LBP computes the local gray scale difference by comparing it with each of its neighbor pixel(s) in a selected radius of R. A zero is assigned when the difference is less than zero and in remaining values it is taken as 1. A decimal number is computed using these thresholds in the encoding step. The LBP operator (Ojala *et al*., 2002) for a given pixel of the image is as follows:

$$LBP_{P,\ R} = \sum_{p\ =\ 0}^{P-1} s\left(g_p - g_c\right)2^p,\ s\left(x\right) = \begin{cases} 1,\ x \geq 0 \\ 0,\ x < 0 \end{cases} \tag{1}$$

where, g_c and g_p are the gray values of centre pixel and its neighbors. P is the maximum number of neighbors in the selected neighborhood of radius R. The coordinates of g_p are (-Rsin (2πp/P), Rcos (2πp/P)) when the coordinates of g_c is (0,0). A histogram is to be calculated to represent the texture of the image after computing the LBP coding for each pixel of the image. The two steps of LBP operator is shown in Fig. 1.

The intensity values g_p (p = 0, ..., p-1) move correspondingly along with the perimeter of the circle around (g_0) when the image is in rotation. While rotating a particular binary pattern, different LBP values are obtained, g_0 is assigned to the right of g_c with a gray value of element (0,R) where as single LBP value is obtained with rotation invariant LBP. The rotation invariant LBP (Ojala *et al*., 2002) is defined as follows:

$$LBP^{ri}_{P,R} = \min\left\{\left(ROR\left(LBP_{P,R},\ i\right)\right|\ i = 0,1,\ldots,P-1\right)\right\} \tag{2}$$

where, ROR (x, i) performs a circular bit-wise right shift on the P-bit number x, i times. Ojala *et al*. (2002) have developed uniform patterns to minimize the vast majority pattern in local binary pattern. The uniform values for LBP (Ojala *et al*., 2002) are defined as the number of bitwise transitions in the pattern as follows:

$$U\left(LBP_{P,R}\right) = \left|s\left(g_{P-1} - g_c\right) - s\left(g_0 - g_c\right)\right| + \sum_{p=1}^{P-1}\left|s\left(g_p - g_c\right) - s\left(g_{p-1} - g_c\right)\right| \tag{3}$$

where g_c, g_p, P are defined as in Eq. 1. The uniform pattern ($U(LBP_{P,R})$) is a pattern with transitions not >2. For example, the patterns are 11111111 (zero bitwise change), 00000111 (two bitwise changes), 10001000 (four bitwise changes) and 01010101 (eight bitwise changes). In these patterns first two patterns are uniform because only <=2 transitions (bitwise changes) can be found and third and fourth are not uniform.

Rotation invariance has a significant role in texture classification. So, the rotation invariant LBP is combined with uniform patterns (Ojala *et al*., 2002a, b). Rotation invariant and uniform local binary pattern is described as follows:

$$LBP^{riu2}_{P,R} = \begin{cases} \sum_{p=0}^{P-1} s(g_p - g_c), \text{if } U(LBP_{P,R} \le 2) \\ P+1, \text{otherwise} \end{cases} \quad (4)$$

where, g_c, g_p, P are defined as in Eq. 1. The mapping from $LBP_{P,R}$ to $LBP^{riu2}_{P,R}$ which has P+2 distinct output values, can be implemented with a lookup table of elements (Ojala *et al*., 2002a, b).

$LBP^{riu2}_{P,R}$ is invariant to gray scale values, thus, it discards the contrast. The contrast of image is required without gray-scale invariant, the local variance (VAR) (Ojala *et al*., 2002) of image is proposed. It is defined as follows:

$$VAR_{P,R} = \frac{1}{P}\sum_{p=0}^{P-1}(g_p - \mu)^2 \text{ where } \mu = \frac{1}{P}\sum_{p=0}^{P-1} g_p \quad (5)$$

Here, g_c, g_p P are defined as in Eq.(1). $LBP^{riu2}_{P,R}$ and VAR complement with each other, based on contrast. The joint distribution of $LBP^{riu2}_{P,R}$ and VAR ($LBP^{riu2}_{P,R}$/VAR) became a powerful rotation invariant measure.

Local ternary pattern: Usage of central pixel as a threshold in local binary pattern made LBP sensitive to noise method, mainly in the near uniform image regions. A small change of the central pixel (60-65) greatly changes the LBP code and is shown in Fig. 2. To overcome the disadvantage, Local Ternary Pattern (LTP) (Tan and Tringgs, 2010) has been developed. The LTP operator is defined as follows:

$$LTP_{P,R} = \sum_{p=0}^{P-1} s(g_p - g_c)2^p, s(x) = \begin{cases} 1, & x \ge t \\ 0, & -t < x < t \\ -1, & x \le -t \end{cases} \quad (6)$$

where, g_c, g_p, P are defined as in Eq. 1 and t is a threshold, defined by user. Conventional 2-valued (0,1) LBP code is extended to 3-valued (-1, 0,1) ternary code by using threshold t and pictorially presented in Fig. 3. The ternary code made the LTP insensitive to noise but it is no longer invariant to monotonic gray scale transformation.

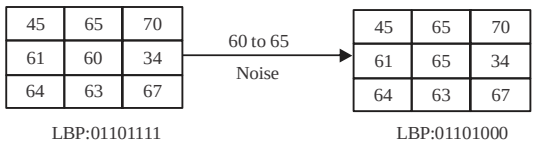

Fig. 2: Example for LBP is noise sensitive

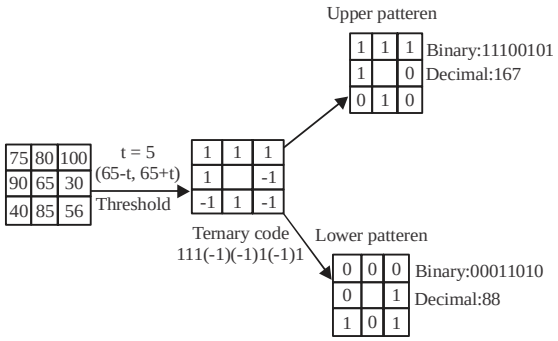

Fig. 3: Example for LTP Process

In Fig. 3 ternary code is 111(-1)(-1)1(-1)1, the binary code for upper pattern is 11100101, the binary code for lower pattern is 00011010. The followed thresholding step, encode the upper pattern and lower pattern and build the histograms for upper LTP and lower LTP. Finally, LTP operator is constructed with the concatenation of histograms of upper LTP and lower LTP.

Completed Local Binary Pattern (CLBP): The CLBP (Guo *et al*., 2010) improves the capability of LBP by decomposing the image local differences into two complementary components signs (s_p) and magnitudes (m_p) and are defined as follows:

$$s_p = s(g_p - g_c),\ m_p = |g_p - g_c| \quad (7)$$

where, g_c, g_p are defined as in Eq. 1. CLBP is defined with a set of three operators, CLBP_S, CLBP_M and CLBP_C. Among the three operators CLBP_S is as same as LBP and is illustrated in Fig. 4. CLBP_M provides the local variance of magnitude. It is shown in Fig. 5 and is defined as follows:

$$CLBP\_M_{P,R} = \sum_{p=0}^{P-1} t(m_p, c)2^p,\ t(x,c) = \begin{cases} 1, & x \ge c \\ 0, & x < c \end{cases} \quad (8)$$

where, c is the mean value of m_p of the whole image and g_c, g_p are as described in Eq. 1. CLBP_C operator provides the local central information. It is defined as follows:

$$CLBP\_C_{P,R} = s(g_c - c_l) \quad (9)$$

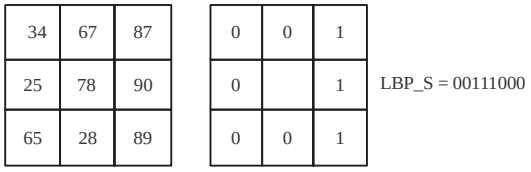

Fig. 4: LBP_S operator

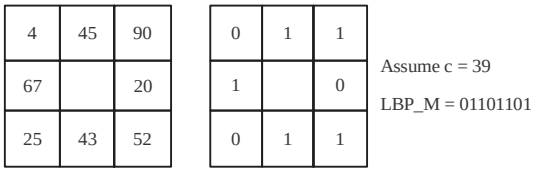

Fig. 5: LBP_M operator

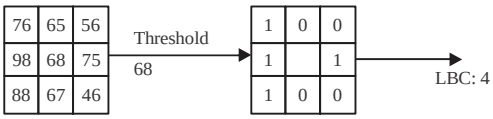

Fig. 6: LBC operator

Here, c_l is the average gray level of whole image. A significant improvement for rotation invariant texture classification accuracy is obtained by combining the three operators (Guo *et al*., 2010).

Completed local binary count: Experimentally it is found that the number of specified rotation invariant structural patterns is too few to contain abundant structural information. It is also observed that some rotation invariant patterns of LBP may change after rotation and interpolation (Zho *et al*., 2010). As a solution, LBC is developed and further it is enhanced to CLBC (Zho *et al*., 2010) for improved performance in classification of textures. Local binary count is defined as follows:

$$LBC_{P,R} = \sum_{p=.}^{P-1} s(g_p - g_c),\ s(x) = \begin{cases} 1, & x \geq 0 \\ 0, & x < 0 \end{cases} \quad (10)$$

where, g_c, g_p P are defined as in Eq. 1. LBC totally avoids the microstructure information. The illustration is given in Fig. 6. LBC has been extended to completed LBC (CLBC) with three operators CLBC_S, CLBC_M and CLBC_C. The three operators can be combined either jointly or hybridly like CLBP. CLBC_S is same as LBC. CLBC_M and CLBC_C are defined as follows:

$$CLBC\_M_{P,R} = \sum_{p=0}^{P-1} t(m_p, c),\ t(x,c) = \begin{cases} 1, & x \geq c \\ 0, & x < c \end{cases} \quad (11)$$

where, c denotes the mean value of m_p in the whole image and mp = $|g_p - g_c|$:

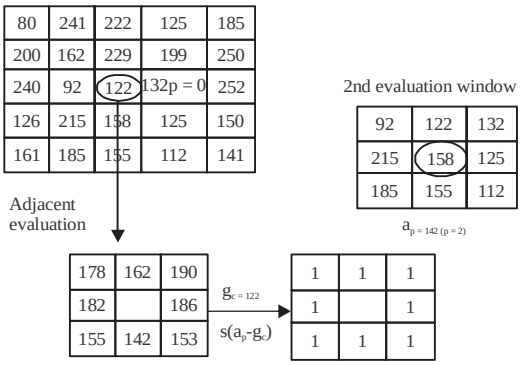

Fig. 7: AELBP operator

$$CLBC\_C_{P,R} = s(g_c - c_l) \quad (12)$$

where, g_c, g_p, P are described as in Eq. 1. c_l is the average gray level of whole image.

Adjacent evaluation local binary pattern: As conventional LBP is sensitive to noise, AELBP (Song *et al*., 2015) has been developed which is robust to noise. AELBP generates an evaluation window to each neighbor around the neighborhood centreand a value of a_p is calculated at each neighbor. AELBP computes the local binary code by comparing g_c and a_p. It is defined as follows:

$$AELBP_{P,R} = \sum_{p=0}^{P-1} s(a_p - g_c)2^p,\ s(x) = \begin{cases} 1, & x \geq 0 \\ 0, & x < 0 \end{cases} \quad (13)$$

where, g_c is defined as in Eq. 1, P is number of neighborhood pixels and a_p is mean value of p^{th} evaluation window excluding the value of evaluation center and R is radius. The process of AELBP is as follows:

Calculation of a_p: An evaluation window of size WXW (W is odd numbers) is set to each neighbors of the neighborhood center. The value of a_p is computed at each neighbors g_p of the neighborhood center g_c with mean value of gray values in the p^{th} evaluation window excluding the value of center g_p. If window size W is one then AELBP is identical to LBP.

Coding the local binary pattern: LBP can characterize the encoding step based on the difference of a_p and g_c values after completing the thresholding step.

The difference between LBP and AELBP is in the computation of thresholding step. That is in LBP the central pixel g_c is compared with its neighborhood pixel g_p with radius R where as in AELBP, the central pixel g_c is compared with its neighbor a_p with radius R. It is described as in Fig. 7.

Adjacent evaluation completed local binary pattern: Similar to CLBP, it is enhanced to AECLBP (Adjacent evaluation completed local binary pattern). AECLBP is divided into two components, sign component (s_p) and magnitude component (m_p). They are described as follows:

$$s_p = s(a_p - g_c),\ m_p = |a_p - g_c| \tag{14}$$

AECLBP has AECLBP_S, AECLBP_M and AECLBP_C operators. AECLBP_S is equivalent to conventional AELBP. It is shown in Fig. 7. AECLBP_M gives the local variance of magnitude. It is defined as follows:

$$\text{AECLBP\_M}_{P,R} = \sum_{p=0}^{P-1} t(m_p - c)2^p,\ t(x,c) = \begin{cases} 1, & x \geq c \\ 0, & x < c \end{cases} \tag{15}$$

where, c denotes the mean value of m_p in the whole image and g_c, P are described as in Eq. 1, a_p defined in Eq. 13. AECLBP_C operator extracts the local central information. It is defined as follows:

$$\text{AECLBP\_C}_{P,R} = s(g_c - c_I) \tag{16}$$

where, c_I is the average gray level of whole image. A significant improvement for rotation invariant texture classification is obtained by combining these three operators (AECLBP_S, AECLBP_M, AECLBP_C) (Guo *et al*., 2010).

Adjacent evaluation local ternary pattern: Adjacent Evaluation Local Ternary Pattern (AELTP) is proposed by extending binary values (0,1) of AELBP into ternary values (-1,0,1). It is defined as follows:

$$\text{AELTP}_{P,R} = \sum_{p=0}^{P-1} s(a_p - g_c)2^p,\ s(x) = \begin{cases} 1, & x \geq t \\ 0, & -t < x < t \\ -1, & x \leq -t \end{cases} \tag{17}$$

where, t is a threshold and a_p, , g_p, g_c, P, R defined as in Eq. 13 and 1. The difference between LTP and AELTP is the central pixel which is compared with a_p in AELTP. But in LTP central pixel is compared with g_p.

RESULTS AND DISCUSSION

Experiments are conducted to study the performance of existing above said texture descriptor methods using three bench mark huge datasets. They are Outexdatabase (Ojala *et al*., 2002a, b), CUReT database (Dana *et al*., 1999) and UIUC database (Lazebnik *et al*., 2005).

Dissimilarity measuring framework: Various metrics are proposed for measuring the dissimilarity between two histograms such as a histogram intersection, log-likelihood ratio and chi-square statistics. Thus, chi-square statistics (Guo *et al*., 2010; Zho *et al*., 2010) is used. The distance between two histograms H = h_i and K = k_i where (i = 1, 2, 3, ---B) can be defined mathematically as follows:

$$\text{Dissimilarity}_{\chi^2}(H,K) = \sum_{i=1}^{B} \frac{(h_i - k_i)^2}{h_i + k_i} \tag{18}$$

In this research, the nearest neighborhood classifier is used for classification. The complete details of the three databases furnished as follows.

Outex database: Outex_TC_0010(TC10) and Outex_ TC_0012(TC12) are used for the experimentation. The TC10 and TC12 contain 24 classes of texture images. These were collected under three illuminations ("horizon", "inca" and "t184") and nine various rotation angles (0^0, 5^0, 10^0, 15^0, 30^0, 45^0, 60^0, 75^0 and 90^0). Each class has 20 non overlapping 128×128 texture images under each situation.

For TC10, 480 images from this data set are used as training data. These are the images of each class under "inca" illumination with "0^0" rotation of angle. The remaining images from the same data set 3840 are used as testing data. The testing data is images of each class under same illumination with remaining rotation of angles (5^0, 10^0, 15^0, 30^0, 45^0, 60^0, 75^0 and 90^0).

For TC12, The data of TC10 is taken as trained data. Images under 't184' or 'horizon' illumination of TC12 are used for testing. The experimental results of TC10, TC12 (t184), TC12 (horizon) are shown in Table 1.

CUReT database: The CUReT database contains 61 classes of textures retrieved at various viewpoints and illumination orientations. Each class has 92 images. As in (Guo *et al*., 2010; Zho *et al*., 2010) N images for each class are randomly selected as train data and remaining (92-N) images for each class are selected as test data. Experimental results of classification accuracy for N = 6, 12, 23 and 46 is demonstrated in Table 2.

UIUC database: UIUC database contains 25 classes. Each class has 40 images with resolution of 640×480. These images are captured under significant viewpoint variations. N images for each class are randomly selected as train data and remaining (40-N) images for each class are selected as test data for classification (Guo *et al*., 2010; Zho *et al*., 2010). Experimental results for N = 5, 10, 15 and 20 is presented in Table 3.

Table 1: Classification rates (%) on TC10 and TC12 database

	R = 1 P = 8				R = 2 P = 16				R = 3 P = 24			
		TC12				TC12				TC12		
	TC10	t184	Horizon	Average	TC10	t184	Horizon	Average	TC10	t184	Horizon	Average
LTP	94.14	75.88	73.96	81.33	96.95	90.16	86.94	91.35	98.2	93.59	89.42	93.74
LBP^{riu2}	84.81	65.46	63.68	71.32	89.40	82.27	75.21	82.29	95.08	85.05	80.79	86.97
LBP^{ri}	78.8	71.97	69.98	73.58	91.72	88.26	88.47	89.48	-	-	-	-
VAR	88.39	61.48	62.34	70.74	86.61	63.26	68.94	72.94	-	-	-	-
LBP^{riu2}/VAR	95.63	75.93	74.91	82.16	97.08	84.40	83.19	88.22	-	-	-	-
CLBP_S	84.81	65.46	63.68	71.32	89.40	82.27	75.21	82.29	95.08	85.05	80.79	86.97
CLBC_S	82.94	65.02	63.17	70.38	88.67	82.57	77.41	82.88	91.35	83.82	82.75	85.97
AECLBP_S	82.34	73.68	68.71	74.91	90.29	83.54	78.52	84.12	89.92	83.29	81.06	84.76
CLBP_M	81.74	59.30	62.77	67.94	93.67	73.79	72.40	79.95	95.52	81.18	78.65	85.12
CLBC_M	78.96	53.63	58.01	63.53	92.45	70.35	72.64	78.48	91.85	72.59	74.58	79.67
AECLBP_M	83.62	66.55	63.50	71.22	86.67	73.13	75.14	78.31	92.86	73.96	78.91	81.91
CLBP_S_M	94.66	82.75	83.14	86.85	97.89	90.55	91.11	93.18	99.32	93.58	93.35	95.42
CLBC_S_M	95.23	82.12	83.59	86.98	98.10	89.95	90.42	92.82	98.70	91.41	90.25	93.45
AECLBP_S_M	95.49	87.38	88.13	90.33	97.89	91.88	91.83	93.87	99.01	93.80	93.91	95.57
CLBP_S_M_C	96.56	90.30	92.29	93.05	98.72	93.54	93.91	95.39	98.93	95.32	94.53	96.26
CLBC_S_M_C	97.16	89.79	92.92	93.29	98.54	93.26	94.07	95.29	98.78	94.00	93.24	95.34
AECLBP_S_M_C	97.58	91.83	91.81	93.74	98.80	95.42	94.70	96.31	99.19	96.83	95.05	97.02
AELTP	92.73	79.14	76.34	82.74	96.69	89.24	86.41	90.78	97.55	91.30	88.45	92.43

Table 2: Classification rates (%) on CUReT database

	R = 1 P = 8				R = 2 P = 16				R = 3 P = 24			
	6	12	23	46	6	12	23	46	6	12	23	46
LTP	65.17	74.61	80.85	87.74	68.72	80.18	86.17	91.16	72.76	82.42	87.19	91.52
LBP^{riu2}	60.36	69.05	74.64	81.32	63.38	72.70	79.28	84.53	67.86	75.51	81.65	86.35
LBP^{ri}	66.60	75.10	80.47	86.06	68.34	75.27	80.61	85.21	-	-	-	-
VAR	43.27	49.63	55.55	61.72	41.16	45.31	50.61	55.95	-	-	-	-
LBP^{riu2}/VAR	71.56	80.90	86.96	92.91	73.20	81.60	88.19	94.23	-	-	-	-
CLBP_S	60.36	69.05	74.64	81.32	63.38	72.70	79.28	84.53	67.86	75.51	81.65	86.35
CLBC_S	58.81	66.76	72.61	77.76	60.24	67.79	73.63	79.00	61.95	68.05	73.79	77.69
AECLBP_S	58.43	65.78	71.82	77.94	62.83	72.30	78.31	83.14	65.19	73.69	80.26	85.42
CLBP_M	54.19	60.77	67.21	75.73	59.60	68.25	76.52	81.32	64.86	71.43	80.42	87.31
CLBC_M	45.06	50.98	56.33	64.33	50.27	59.49	65.91	71.53	52.23	59.26	69.11	75.20
AECLBP_M	56.58	65.49	72.46	77.48	60.79	69.84	79.62	84.43	65.23	74.02	81.16	86.64
CLBP_S_M	74.41	82.90	88.90	92.62	76.47	84.32	89.92	93.30	77.90	84.73	90.99	93.97
CLBC_S_M	72.17	80.82	87.00	91.59	73.79	81.78	89.36	93.30	72.84	80.76	88.29	93.01
AECLBP_S_M	73.69	82.40	89.67	93.23	76.25	83.77	90.45	94.01	77.22	85.76	91.04	95.12
CLBP_S_M_C	76.82	84.96	91.54	95.33	78.07	86.45	92.30	95.40	78.99	86.37	92.51	95.90
CLBC_S_M_C	75.09	83.32	90.66	94.23	76.65	84.12	92.42	95.15	76.00	83.38	91.35	95.01
AECLBP_S_M_C	77.07	84.84	91.90	94.94	78.50	86.11	92.61	95.72	79.03	87.03	92.61	96.54
AELTP	67.12	76.76	84.20	89.27	71.27	80.51	86.89	90.77	72.04	81.19	87.57	91.87

Table 3: Classification rates (%) on UIUC database

	R = 1 P = 8				R = 2 P = 16				R = 3 P = 24			
	5	10	15	20	5	10	15	20	5	10	15	20
LTP	50.06	58.27	64.64	67.80	61.26	71.33	74.40	78.20	60.91	74.53	78.72	83.40
LBP^{riu2}	41.02	49.20	52.16	56.40	41.25	52.00	58.08	57.20	45.25	56.26	59.84	64.60
LBP^{ri}	43.89	50.80	57.12	63.20	49.26	60.67	66.56	71.80	-	-	-	-
VAR	36.34	43.73	47.84	49.80	39.20	47.33	50.40	51.00	-	-	-	-
LBP^{riu2}/VAR	51.77	63.07	67.84	67.80	58.86	67.33	71.04	73.80	-	-	-	-
CLBP_S	41.02	49.20	52.16	56.40	41.25	52.00	58.08	57.20	45.25	56.26	59.84	64.60
CLBC_S	40.00	48.80	51.36	56.80	42.17	54.27	58.56	62.00	48.34	59.87	62.72	67.80
AECLBP_S	37.71	48.13	54.40	57.40	42.51	51.06	59.04	60.60	46.63	57.07	61.44	62.40
CLBP_M	40.45	52.26	55.84	57.40	58.17	66.00	69.92	72.40	58.40	67.33	71.52	76.40
CLBC_M	40.57	46.26	49.60	53.40	51.09	60.00	65.92	69.80	54.17	61.07	67.84	70.00
AECLBP_M	45.94	57.47	58.08	61.80	56.00	66.80	67.36	72	60.57	68.40	71.36	75.40
CLBP_S_M	66.05	75.86	80.48	83.80	73.14	82.00	85.76	88.60	75.08	84.26	86.40	90.00
CLBC_S_M	66.17	75.47	80.00	82.80	76.11	82.67	86.24	89.80	76.46	86.67	87.36	89.80
AECLBP_S_M	67.77	76.80	82.08	86	72.57	82.26	86.40	88.80	78.17	85.73	88.32	92.20
CLBP_S_M_C	75.20	84.93	86.08	88.20	81.26	86.40	89.12	92.20	79.65	87.06	87.52	93.00
CLBC_S_M_C	75.43	85.47	86.88	88.60	80.69	87.20	88.16	92.60	81.02	86.80	89.28	92.40
AECLBP_S_M_C	78.17	84.40	85.28	89.80	80.46	88.53	87.84	92	82.97	89.07	91.2	94.20
AELTP	50.86	61.6	62.88	69.2	64.91	71.33	73.28	79.60	63.89	75.73	77.60	82.80

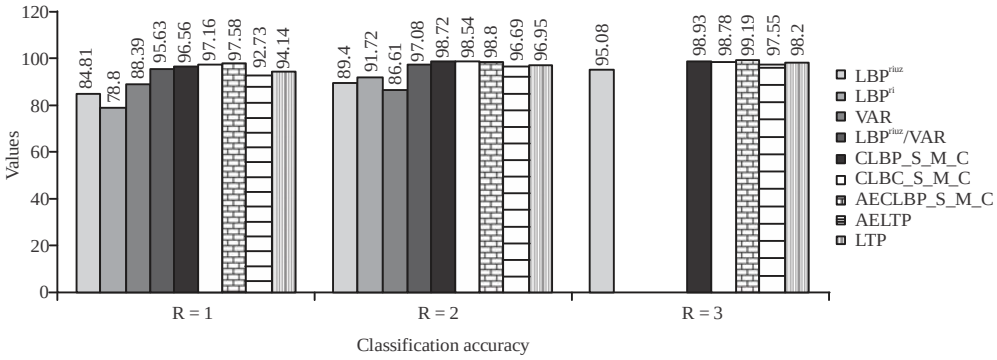

Fig. 8: Comparison of the classification accuracy (%) of LBP variants on TC10 database with R = 1, 2 and 3

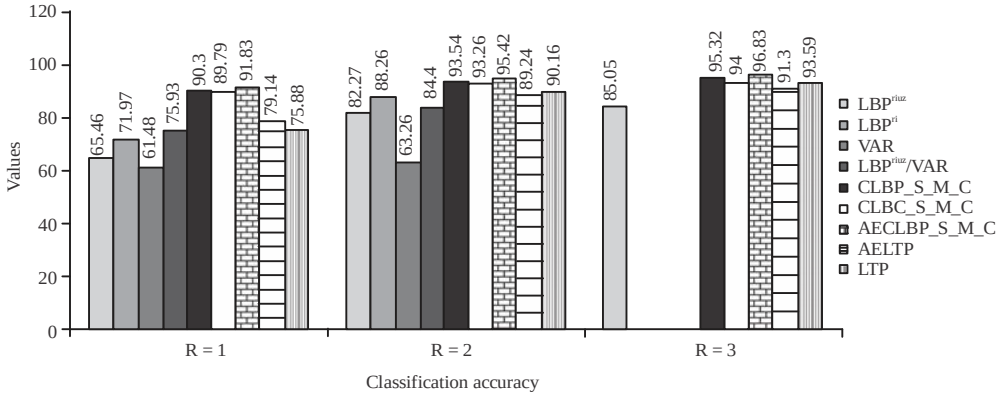

Fig. 9: Comparison of the classification accuracy (%) of LBP variants on TC12 (t184) database with R = 1, 2 and 3

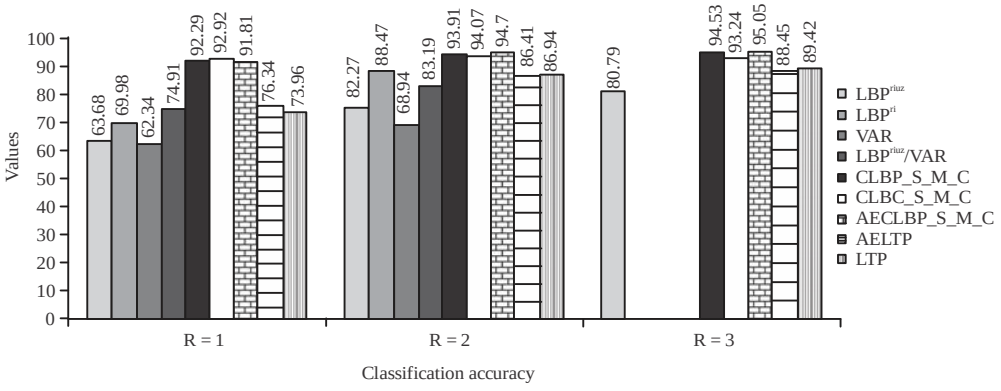

Fig. 10: Comparison of the classification accuracy (%) of LBP variants on TC12 (horizon) database with R = 1, 2 and 3

LBP variant methods are validated using classification performance. It is defined by using formula:

$$\text{Classification performance} = \frac{N_{right}}{M} \times 100 \qquad (19)$$

where, N_{right} is the number of right classifications and M is number of images in test data. The findings of the study on classification performance of LBP variants are provided as follows:

Discussions: We have tested on three bench mark databases Outex, CUReT, UIUC. The details of results are described as:

Outex: The performance of classification accuracy on TC10, TC12 (t184) and TC12 (horizon) for radius R = 1, 2 and 3 is shown in Fig. 8-10. In average AECLBP_S_M_C has achieved classification accuracy 93.74, 96.31 and 97.02% for radius R = 1, 2 and 3. It is better when compared to local binary pattern variants (LBP^{riu2}, LBP^{ri}, VAR, LBP^{riu2}/VAR, CLBP_S_M_C, CLBC_S_M_C, AELTP, LTP).

The classification accuracy on CUReT database with train data N = 6, 12, 23 and 46 textures from each class with radius R = 1, 2 and 3 is illustrated in Fig. 11-14.

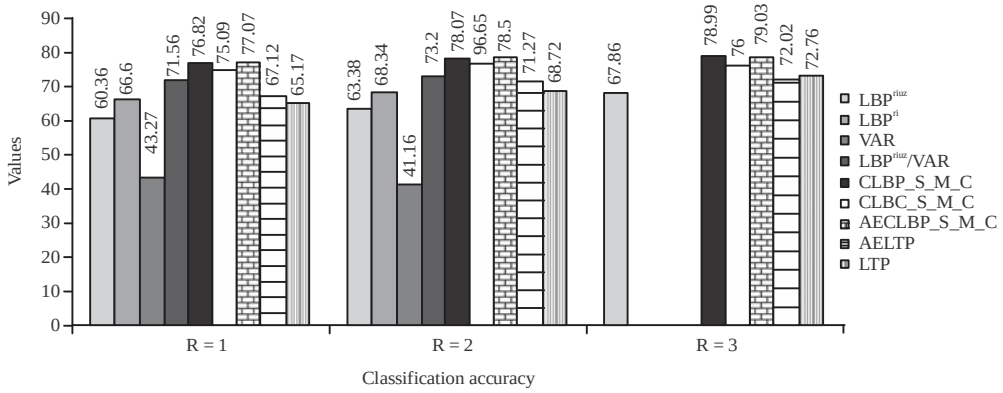

Fig. 11: Comparison of classification accuracy (%) of LBP variants on CUReT database for N = 6 with radius R = 1, 2 and 3

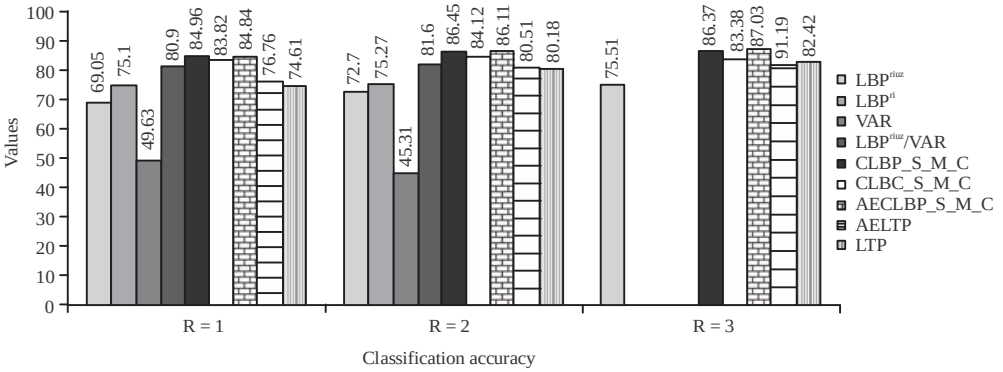

Fig. 12: Comparison of classification accuracy (%) of LBP variants on CUReT database for N = 12 with radius R = 1, 2 and 3

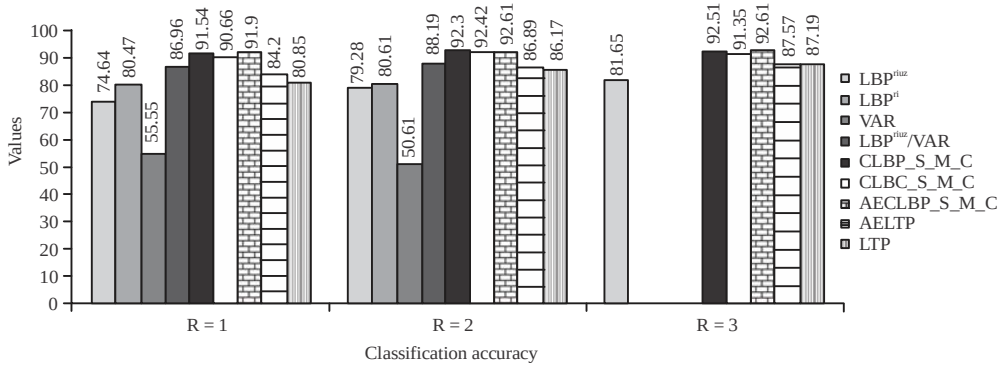

Fig. 13: Comparison of classification accuracy (%) of LBP variants on CUReT database for N = 23 with radius R = 1, 2 and 3

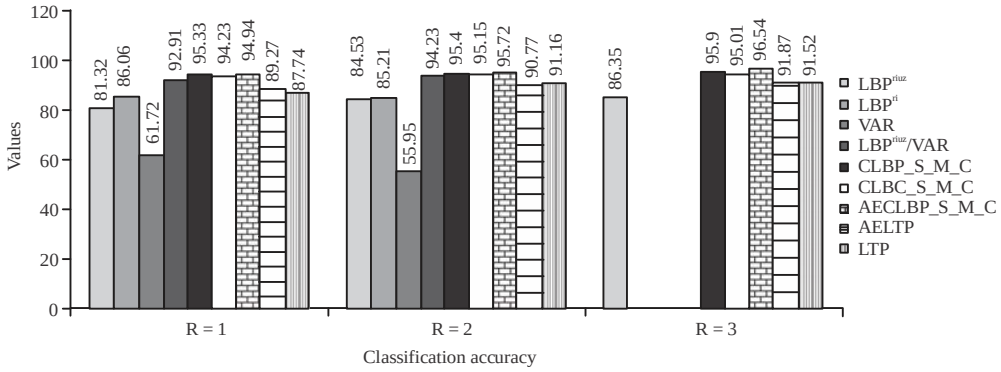

Fig. 14: Comparison of classification accuracy (%) of LBP variants on CUReT database for N = 46 with radius R = 1, 2 and 3

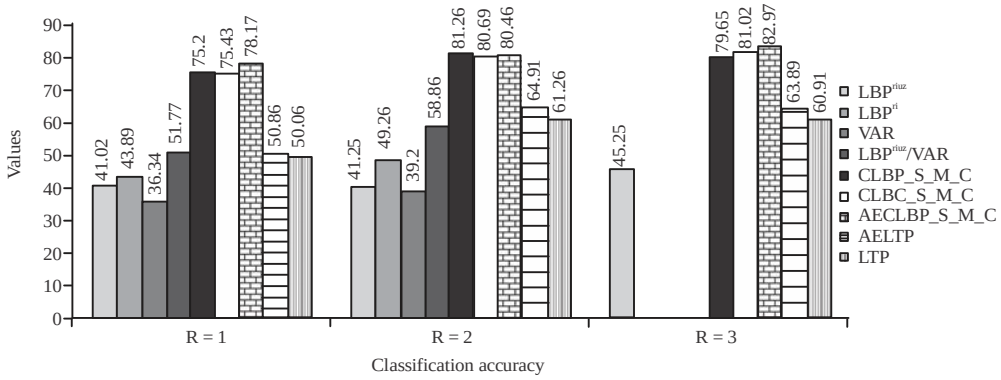

Fig. 15: Comparison of classification accuracy (%) of LBP variants on UIUC database for N = 5 with radius R = 1, 2 and 3

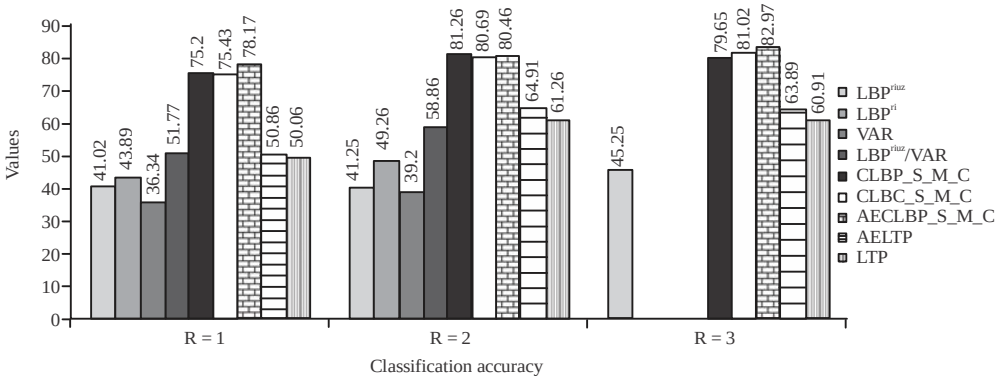

Fig. 16: Comparison of classification accuracy (%) of LBP variants on UIUC database for N = 10 with radius R = 1, 2 and 3

In average AECLBP_S_M_C is achieved better classification accuracy compared to LBP^{riu2}, LBP^{ri}, VAR, LBP^{riu2}/VAR, CLBP_S_M_C, CLBC_S_M_C, AELTP, and LTP.

UIUC: The performance of classification accuracy on CUReT database with train data N = 5, 10, 15 and 20 textures from each class with radius R = 1, 2 and 3 is illustrated in Fig. 15-18. In average AECLBP_S_M_C has achieved better classification accuracy compared to LBP^{riu2}, LBP^{ri}, VAR, LBP^{riu2}/VAR, CLBP_S_M_C, CLBC_S_M_C, AELTP and LTP.

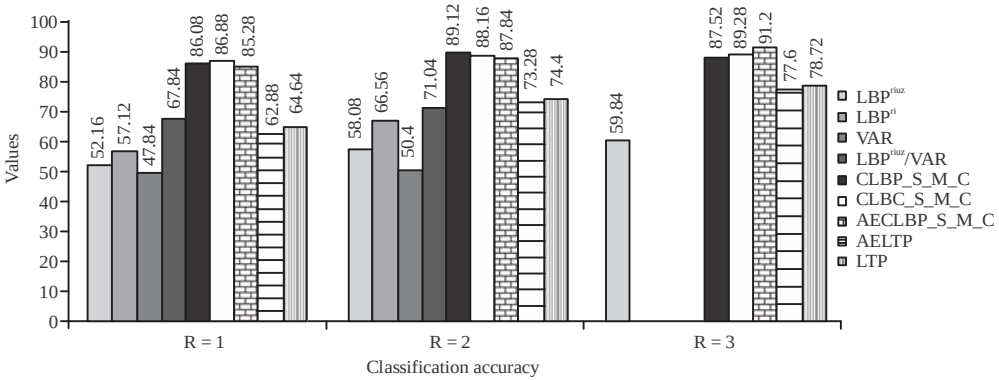

Fig. 17: Comparison of classification accuracy (%) of LBP variants on UIUC database for N = 15 with radius R = 1, 2 and 3

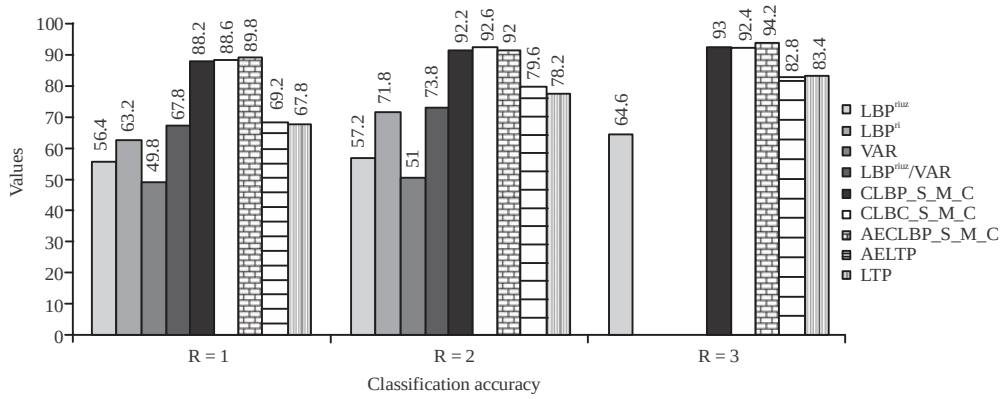

Fig. 18: Comparison of classification accuracy (%) of LBP variants on UIUC database for N = 20 with radius R = 1, 2 and 3

CONCLUSION

This study studied the performance of various rotation invariant LBP variants (LBP^{riu2}, LBP^{ri}, VAR, LBP^{riu2}/VAR, CLBP, CLBC, AECLBP, LTP, AELTP applying on three huge data sets. Among these LBP^{riu2}, LBP^{ri}, LBP^{riu2}/VAR, CLBP and CLBC are noise sensitive and AECLBP, LTP, AELTP are robust to noise. In average AECLBP performs well when compared to all other noise insensitive texture methods. CLBP, CLBC performs well in classification among the noise sensitive texture methods. But from the literature, the number of noise insensitive methods is very few and there is a need to develop noise insensitive methods for many texture classification applications. Developing new noise insensitive texture classification methods is out future endeavor.

REFERENCES

Ahonen, T., A. Hadid and M. Pietikainen, 2006. Face description with local binary patterns: Application to face recognition. IEEE Trans. Pattern Anal. Mach. Intell., 28: 2037-2041.

Cohen, F.S., Fan, Z. and M.A. Patel, 1991. Classification of rotated and scaled textured images using gaussian markov random field models. IEEE Trans. Pattern Anal. Machine Intel., 13: 192-202.

Dana, K.J., B. Van Ginneken, S.K. Nayar and J.J. Koenderink, 1999. Reflectance and texture of real-world surfaces. ACM Trans. Graphics (TOG), 18: 1-34.

Davis, L.S., S.A. Johns and J.K. Aggarwal, 1997. Texture analysis using generalized co-occurrence matrices. IEEE. Trans. Pattern Anal. Mach. Intell., 1: 251-259.

Duvernoy, J., 1984. Optical-digital processing of directional terrain textures invariant under translation, rotation and change of scale. Applied Optics, 23: 828-837.

Eichmann, G. and T. Kasparis, 1988. Topologically invariant texture descriptors. Comput. Vision Graphics Image Process., 41: 267-281.

Goyal, R.K., W.L. Goh, D.P. Mital and K.L. Chan, 1995. Scale and rotation invariant texture analysis based on structural property. Proceedings of the Proceedings of IECON'95-21st Annual Conference on IEEE Industrial Electronics Vol. 2, November 6-10, 1995, IEEE, Orlando, Florida, pp: 1290-1294.

Greenspan, H., S. Belongie, R. Goodman and P. Perona, 1994. Rotation invariant texture recognition using a steerable pyramid. Proceedings of the 12th IAPR International Conference on Pattern Recognition Vol. 3-Conference C: Signal Processing (Cat. No. 94CH3440-5), October 9-13, 1994, IEEE, Jerusalem, Israel, pp: 162-167.

Guo, Z., L. Zhang and D. Zhang, 2010. A completed modeling of local binary pattern operator for texture classification. IEEE Trans. Image Process., 19: 1657-1663.

Hen, Y.W., M. Khalid and R. Yusof, 2007. Face verification with Gabor representation and support vector machines. Proceedings of the 1st Asia International Conference on Modelling & Simulation (AMS'07), March 27-30, 2007, IEEE, Phuket, Thailand, pp: 451-459.

Hu, M.K., 1962. Visual pattern recognition by moment invariants. IRE Trans. Inform. Theor., 8: 179-187.

Huang, X., S.Z. Li and Y. Wang, 2004. Shape localization based on statistical method using extended local binary pattern. Proceedings of the 3rd International Conference on Image and Graphics (ICIG'04), December 18-20, 2004, IEEE, Hong Kong, China, pp: 184-187.

Kashyap, R.L. and A. Khotanzad, 1986. A model-based method for rotation invariant texture classification. IEEE Trans. Pattern Anal. Mach. Intell., 4: 472-481.

Lam, W.K. and C.K. Li, 1997. Rotated texture classification by improved iterative morphological decomposition. IEE. Proc. Vision Image Signal Process., 144: 171-179.

Lazebnik, S., C. Schmid and J. Ponce, 2005. A sparse texture representation using local affine regions. IEEE Trans. Pattern Anal. Mach. Intell., 27: 1265-1278.

Lepisto, L., L. Kunttu, J. Autio and A. Visa, 2003. Rock image classification using non-homogenous textures and spectral imaging. Proceedings of the 11th International Conference in Central Europe on Computer Graphics, Visualization and Computer (WSCG‘03), February 3-7, 2003, Plzen, Czech Republic, pp: 82-86.

Ojala, T., M. Pietikainen and T. Maenpaa, 2002a. Multiresolution gray-scale and rotation invariant texture classification with local binary patterns. IEEE Trans. Pattern Anal. Mach. Intell., 24: 971-987.

Ojala, T., T. Maenpaa, M. Pietikainen, J. Viertola, J. Kyllonen and S. Huovinen, 2002b. Outex-A new framework for empirical evaluation of texture analysis algorithms. Proceedings of the 16th International Conference on Pattern Recognition, August 11-15, 2002, Quebec, Canada, pp: 701-706.

Rassem, T.H. and B.E. Khoo, 2014. Completed local ternary pattern for rotation invariant texture classification. Sci. World J., Vol. 2014, 10.1155/2014/373254

Recio, J.A.R., L.A.R. Fernandez and A. Fernandez-Sarria, 2005. Use of gabor filters for texture classification of digital images. Earth Phys., 17: 47-59.

Salem, Y.B. and S. Nasri, 2009. Texture classification of woven fabric based on a GLCM method and using multiclass support vector machine. Proceedings of the 2009 6th International Multi-Conference on Systems, Signals and Devices, March 23-26, 2009, IEEE, Djerba, Tunisia, pp: 1-8.

Shrivastava, N. and V. Tyagi, 2014. An effective scheme for image texture classification based on binary local structure pattern. Visual Comput., 30: 1223-1232.

Song, K., Y. Yan, Y. Zhao and C. Liu, 2015. Adjacent evaluation of local binary pattern for texture classification. J. Visual Commun. Image Represent., 33: 323-339.

Tan, X. and B. Triggs, 2010. Enhanced local texture feature sets for face recognition under difficult lighting conditions. IEEE Trans. Image Proces., 19: 1635-1650.

Tou, J.Y., Y.H. Tay and P.Y. Lau, 2009. A comparative study for texture classification techniques on wood species recognition problem. Proceedings of the 2009 5th International Conference on Natural Computation, Vol. 5, August 14-16, 2009, IEEE, Tianjin, China, pp: 8-12.

Tuceyran, M. and A.K. Jain, 1993. Texture analysis. Handbook Pattern Recognit. Comput. Vision, 2: 235-276.

Zhao, Y., D.S. Huang and W. Jia, 2012. Completed local binary count for rotation invariant texture classification. IEEE Trans. Image Process., 21: 4492-4497.